

# Nuclear Structure Functions in the Large $x$ Large $Q^2$ Kinematic Region in Neutrino Deep Inelastic Scattering

M. Vakili<sup>3</sup>, C. G. Arroyo<sup>4</sup>, P. Auchincloss<sup>9</sup>, L. de Barbaro<sup>7</sup>, P. de Barbaro<sup>9</sup>, A. O. Bazarko<sup>4</sup>, R. H. Bernstein<sup>5</sup>, A. Bodek<sup>9</sup>, T. Bolton<sup>6</sup>, H. Budd<sup>9</sup>, J. Conrad<sup>4</sup>, D. A. Harris<sup>9</sup>, R. A. Johnson<sup>3</sup>, J. H. Kim<sup>4</sup>, B. J. King<sup>4</sup>, T. Kinnel<sup>10</sup>, G. Koizumi<sup>5</sup>, S. Koutsoliotas<sup>4</sup>, M. J. Lam<sup>5</sup>, W. C. Leffmann<sup>1</sup>, W. Marshall<sup>5</sup>, K. S. McFarland<sup>9</sup>, C. McNulty<sup>4</sup>, S. R. Mishra<sup>4</sup>, D. Naples<sup>5</sup>, P. Nienaber<sup>11</sup>, M. J. Oreglia<sup>2</sup>, L. Perera<sup>3</sup>, P. Z. Quintas<sup>4</sup>, A. Romosan<sup>4</sup>, W. K. Sakumoto<sup>9</sup>, B. A. Schumm<sup>2</sup>, F. J. Sciulli<sup>4</sup>, W. G. Seligman<sup>4</sup>, M. H. Shaevitz<sup>4</sup>, W. H. Smith<sup>10</sup>, P. Spentzouris<sup>4</sup>, R. Steiner<sup>1</sup>, E. G. Stern<sup>4</sup>, U. K. Yang<sup>9</sup>, J. Yu<sup>5</sup>

(1) Adelphi University, Garden City, NY 11530 USA;

(2) University of Chicago, Chicago, IL 60637 USA;

(3) University of Cincinnati, Cincinnati, OH 45221 USA;

(4) Columbia University, New York, NY 10027 USA;

(5) Fermi National Accelerator Laboratory, Batavia, IL 60510 USA;

(6) Kansas State University, Manhattan, KS 66506 USA;

(7) Northwestern University, Evanston, IL 60208 USA;

(8) University of Oregon, Eugene, OR 97403 USA;

(9) University of Rochester, Rochester, NY 14627 USA;

(10) University of Wisconsin, Madison, WI 53706 USA;

(11) Xavier University, Cincinnati, OH 45207 USA

Data from the CCFR E770 Neutrino Deep Inelastic Scattering (DIS) experiment at Fermilab contain events with large Bjorken  $x$  ( $x > 0.7$ ) and high momentum transfer ( $Q^2 > 50 \text{ (GeV}^2\text{)}^2$ ). A comparison of the data with a model based on no nuclear effects at large  $x$ , shows a significant excess of events in the data. Addition of Fermi gas motion of the nucleons in the nucleus to the model does not explain the excess. Adding a higher momentum tail due to the formation of "quasi-deuterons" makes some improvement. An exponentially falling  $F_2 / e^{s(x-x_0)}$  at large  $x$ , predicted by "multi-quark clusters" and "few-nucleon correlations", can describe the data. A value of  $s = 8.3 \pm 0.7 \text{ (stat)} \pm 0.7 \text{ (sys)}$  yields the best agreement with the data.

PACS numbers: 13.15+g

(April 13, 2024)

Deep inelastic scattering (DIS) neutrino interactions are ideally suited for measuring the nuclear structure functions over a wide range of kinematic variables. The CCFR experiment has collected over  $10^6$  charged current events where neutrinos and antineutrinos scattered off of an iron target. We have recently published [1] structure functions for the Bjorken  $x$  region of  $x < 0.75$  based on these data. In this paper, we extend the measurement into the  $x > 0.75$  region [2]. We have approximately 2000 events with  $x > 0.75$ .

In the infinite momentum frame,  $x$  is the fraction of the nucleon's momentum carried by the struck quark. As such,  $x$  is kinematically constrained to be less than 1. In the same model, quark counting rules [3] would imply that the quark structure functions should decrease like  $(1-x)^3$  near  $x = 1$ .

When  $x$  is measured in DIS experiments, it is assumed that the incident lepton scatters off a nucleon at rest in the laboratory. Under this assumption and neglecting terms proportional to the nucleon's mass,  $x$  takes on the form

$$x = \frac{2E_1 E_{10}}{M_N E_{\text{had}}} \sin^2 \frac{\theta}{2}; \quad (1)$$

where  $E_1$  is the energy of the incoming lepton,  $E_{10}$  is the energy of the outgoing lepton,  $\theta$  is the laboratory angle between the two leptons,  $E_{\text{had}}$  is the energy of the outgoing hadron shower, and  $M_N$  is the mass of the struck nucleon. However, for nuclear targets (like the iron detector of CCFR) the nucleons need not be at rest in the laboratory. The nucleons themselves have Fermi motion. Furthermore, the quarks inside a given nucleon may be affected by the surrounding nucleons either through the exchange of mesons inside the nucleus, through the formation of few-nucleon states, or through the condensation of the nucleons into multi-quark clusters ("bags"). All of these phenomena have been used to explain the EMC effect [4]. Nuclear motion and quark interactions "smear" out the nucleon's structure functions, taking events from one region in  $x$  and  $Q^2$  and moving them into adjacent regions. In the regions below  $x = 0.75$ , the differences between the nuclear and nucleon structure functions are small mainly because the nucleon structure functions are slowly varying. At  $x = 0.7$ , the nuclear correction is expected to be about 10% [1]. However, in the higher  $x$  region, nucleon structure functions must go to zero while the nuclear structure functions need not. In fact, most of the cross section near  $x = 1$  and all of the cross section

for  $x > 1$  comes from the fact that the quark exists in the nuclear environment. Thus, the high  $x$  region is ideally suited for investigating nuclear effects in DIS scattering.

Event selection in this analysis is very similar to previous CCFR analyses [1,5]. However, because there are so few true high  $x$  events, we are very susceptible to background events from the lower  $x$  region being mis-measured and appearing as high  $x$  events. To minimize this effect, we further restrict the kinematic region for this analysis over previous CCFR analyses to the region where  $x$  is well measured. The resolution of  $x$  is poor at large muon energies, at small hadron energies, and at small muon angles. We also require that the hadronic energy is well contained in the calorimeter and has a small measurement error and that the outgoing muon traverses the whole length of the toroid spectrometer. For these reasons, we require events to be in the kinematic region  $15 \text{ GeV} < E < 360 \text{ GeV}$ ,  $20 < E_{\text{had}} < 360 \text{ GeV}$ ,  $Q^2 < 400 (\text{GeV}/c)^2$ , and  $\theta > 17 \text{ mrad}$ . To minimize the uncertainties from higher twist contributions and from resonant scattering, we accept events where  $Q^2 > 50 (\text{GeV}/c)^2$ . The average  $Q^2$  of the accepted events is  $120 (\text{GeV}/c)^2$ .

In addition to these quality cuts, we made various checks on the muon momentum and hadronic energy measurements. We compared different measurement algorithms and hand-scanned all of the high  $x$  events. There were about 30 events with an apparent discrepancy between two different hadron energy or muon energy measurement algorithms, indicating possible mis-measurements. These events were removed from the sample.

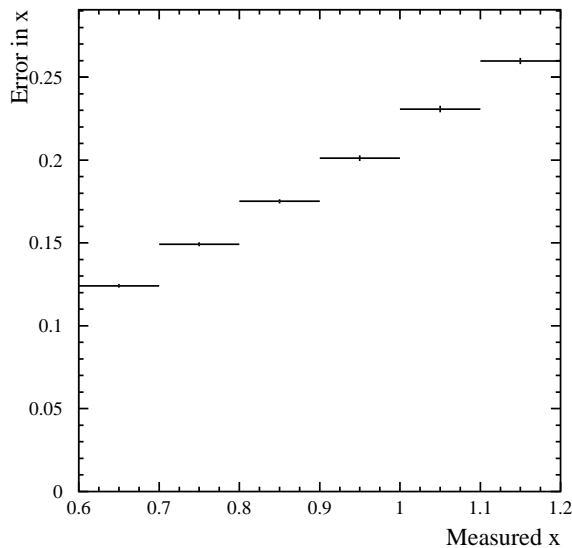


FIG. 1. Error in  $x$  as a function of measured  $x$  in the data.

As with any steeply falling function, the measured distribution is distorted by measurement resolution. In CCFR, the hadron and muon energy resolution functions are measured from test beam data and from internal calibrations [6]. They are well known over four orders of magnitude. An extensive Monte Carlo program has been written to simulate the effects of the detector on neutrino interactions. With this program, we predict the observed  $x$  distribution of a given input model. For models with free parameters, we vary the free parameter until we get the best agreement between the predicted  $x$  distribution and that observed. The  $x$  resolution as a function of  $x$  is shown in Fig. 1. The number plotted is the resolution averaged over the accepted Monte Carlo events.

Neutrino DIS can be completely parameterized (up to effects that are proportional to the muon mass over the neutrino energy) by three structure functions:  $2xF_1$ ,  $F_2$ , and  $xF_3$ . In the quark parton model,  $2xF_1$  and  $F_2$  differ by the distribution of effective scalar partons in the nucleon which arise from the apparent transverse momentum of the quarks. At high  $Q^2$ , the scalar effects are expected to be insignificant.  $2xF_1$  and  $xF_3$  differ by a contribution from sea quarks. At high  $x$ , the sea quark contribution to the structure functions is also negligible. Therefore, for this analysis, we assume that [2], for  $x > 0.6$ ,

$$2xF_1(x; Q^2) = F_2(x; Q^2) = xF_3(x; Q^2): \quad (2)$$

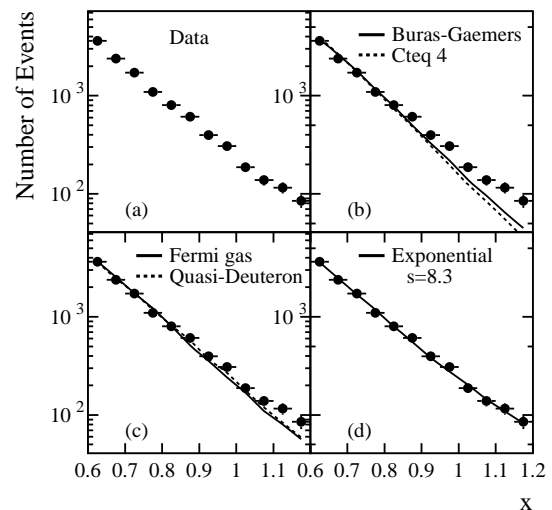


FIG. 2. (a) Measured  $x$  distribution. Comparison of measured  $x$  distribution and (b) distribution predicted by Buras-Gaemers structure functions and by CTEQ 4M structure functions, (c) distributions predicted by a flat Fermi gas model and by the Bodek-Ritchie model, (d) distributions with an exponentially falling  $F_2$  with  $s=8.3$ . All error bars represent only the statistical errors.

As stated above, simple nucleon models of neutrino-

iron scattering do not include the nuclear environment and therefore are not expected to describe our  $x$  distributions. However, it is instructive to compare a model including only nucleon structure functions with our data to see the difference. Fig. 2(a) shows the measured  $x$  distribution from the data. In Fig. 2(b), we show our expected  $x$  distribution generated from the Buras-Gaemers (BG) [7] and from the CTEQ4M parameterizations of the structure functions [8]. The former have been fit to our  $x < 0.7$  data and, as such, include the nuclear effects that are seen at lower  $x$ . Likewise, the latter uses CCFR data in their fits and therefore, to some extent, must include nuclear effects. However, both parameterizations are approximately proportional to  $(1-x)^3$  as  $x$  goes to 1 and therefore do not include high  $x$  nuclear effects. As can be seen in Fig. 2(b), the BG and CTEQ4M parameterizations seriously underestimate the high  $x$  cross section.

When a nuclear Fermi gas model with a Fermi momentum distribution up to a Fermi surface of 257 MeV/c is added to the BG parameterization, the result again underestimates the high  $x$  measurement as shown in Fig. 2(c). It has been found in low energy electron-nucleus scattering measurements and in analyzing the EMC effect in high energy experiments that a high momentum tail has to be added to the pure Fermi gas distribution to reproduce the data. The model of Bodek and Richie [9] introduces the high momentum tail through the inclusion of quasi-deuteron scattering. Fig. 2(c) compares this model with our data. While the comparison with our data is still not perfect, it is slightly better than that for the models with no nuclear motion or with only Fermi motion.

After the discovery of the EMC effect, various more exotic nuclear models were proposed. One such model is the few-nucleon correlation model of Frankfurt and Strikman [10]. Other authors such as Kondratyuk and Shmatikov [11] suggest models where the neutrinos scattered on higher quark-count states (6-quark, 9-quark, etc.). In such models the individual quarks can have a higher effective momentum than in the isolated nucleon. Both the few-nucleon correlation models and the multi-quark cluster models can be parameterized as an exponentially falling  $F_2$  structure function ( $F_2(x) / e^{-sx}$ ) in the large  $x$  region. We have used the parameterized structure function from the BCDMS collaboration [12] and varied the exponential slope parameter  $s$  to minimize the  $\chi^2$  difference between the Monte Carlo prediction and the measured distributions in the region  $0.6 < x < 1.2$ . We find that  $s = 8.3$  minimizes the  $\chi^2$  at 8.2 for 12 degrees of freedom. The region that changes the total  $\chi^2$  by 1 unit leads to an error estimate of  $s = 0.7$ . Fig. 2(d) compares our best exponential fit to the data. Fig. 3 shows  $F_2$  with its error band from this exponential model normalized to the  $x = 0.65$  point from the CCFR structure functions [1].

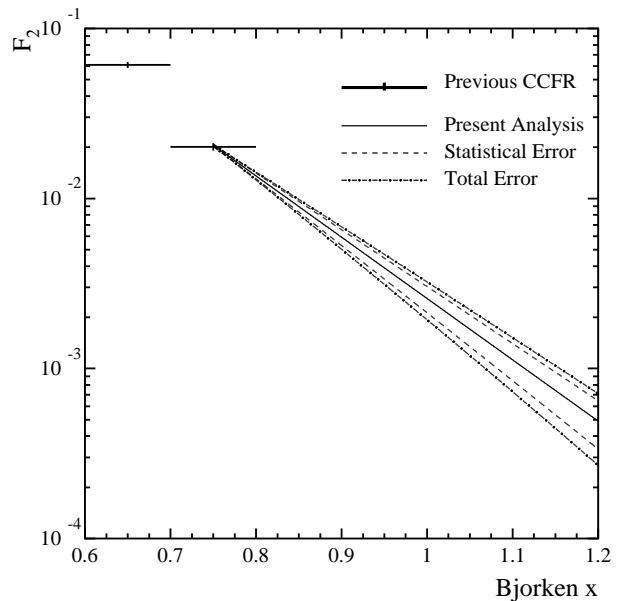


FIG. 3. The exponentially falling  $F_2$  structure function for  $Q^2 = 125 (\text{GeV}/c)^2$  along with the last two points from the previous CCFR analysis. The solid line corresponds to our best fit to an exponential  $F_2$  structure function. The area included by the dashed lines corresponds to the area  $\pm 1$  statistical error around the best fit. The dotted-dashed lines indicate the region allowed by adding both statistical and systematic errors in quadrature. The normalization of this graph is taken from all the data with  $0.6 < x < 0.7$ . The CCFR points plotted are only for the data  $100 (\text{GeV}/c)^2 < Q^2 < 150 (\text{GeV}/c)^2$ .

We have investigated various systematic effects that might affect our determination of the exponential slope parameter. These are given in Table 1. The biggest effect comes from our assumed muon energy resolution. If we broaden or narrow the resolution function from the measured one by one standard deviation, we can change the value of the slope parameter by  $\pm 0.6$ . Other systematic effects, given in Table 1, lead to a total systematic error on the slope parameter of  $\pm 0.7$ . Thus our measured exponential slope parameter is

$$s = 8.3 \pm 0.7 (\text{stat.}) \pm 0.7 (\text{sys.}) \quad (3)$$

Systematic Factor	Error in $s$
Energy scale	0.2
Relative calibration	0.1
Incoming neutrino angle	0.1
Outgoing muon angle	0.1
Hadronic energy measurement	0.1
Radiative corrections	0.1
Muon resolution function	0.6
TOTAL SYSTEMATIC ERROR	0.7

TABLE I. Systematic errors.

Other experiments have measured the exponential slope parameters for nuclear targets in the high  $x$  region. Experiment E133 [13] at SLAC measured the low energy electron-aluminum DIS cross section. Their value of  $s = 7-8$  cannot be directly compared with our result since their high  $x$  events come from the resonance region at low  $Q^2$  and not from the DIS region. The muon-carbon data from BCDMS comes from the DIS region and should be comparable to ours. They find a value of  $s = 16.5 \pm 0.5$  (much steeper slope). This may indicate that the inter-nucleon effects are much greater for our iron target than for their carbon target, although this is not expected theoretically [14]. Recent studies at lower energies [15] from SLAC-NE3 and CEBAF E89-008 have suggested a consistent nuclear picture if  $\sigma = 2x(1 + 1 + \frac{4m_p^2 x^2}{Q^2})$  scaling is used. However, their exponent of approximately  $s = 17$  at  $x = 1$  is inconsistent with our data (in our  $Q^2$  regime,  $x < 1$ ). Our result agrees with the theoretical prediction of  $s = 8-9$  by Strikman and Frankfurt and is larger than the Baklin's prediction [16] of  $s = 6$ .

The model that we used in this analysis assumed a  $Q^2$  dependence of the structure function of  $F_2(x; Q^2) / (Q^2)^{0.18}$ . This dependence is completely compatible with our data.

We thank the staff of the Fermi National Accelerator Laboratory for their hard work in support of this experimental effort. We also wish to thank Mark Strikman and Dong Geesaman for their input on theoretical issues. This research was supported by the U.S. Department of Energy and the National Science Foundation.

- [1] L.A. Kondratyuk, and M. Zh. Shmatikov, *Yad. Fiz.* 41, 22 (1985).
- [2] BCDMS collaboration, *Z. Phys. C* 63, 29 (1994).
- [3] S. Rock, et al., *Compilation of AL/D Ratios in E133 SLAC Experiment*, (1986).
- [4] M. Strikman, private communication.
- [5] J. Arlington, *Inclusive Electron Scattering from Nuclei at  $x > 1$  and High  $Q^2$* , Ph.D. thesis for the California Institute of Technology, 1998 (unpublished); D.H. Potter, *A Measurement of Inclusive Quasielastic Electron Scattering Cross Sections at High Momentum Transfer*, Ph.D. thesis for the California Institute of Technology, 1989 (unpublished); D.B. Day, et al., *Phys. Rev. Lett.* 59, 427 (1987).
- [6] A.M. Baklin, et al., *Sov. J. Nucl. Phys.* 18, 41 (1974).

- 
- [1] W.G. Seligman, et al., *Phys. Rev. Lett.* 79, 1213 (1997).
  - [2] Further details of this analysis can be found in M. Vakil, *A Measurement of the Nuclear Structure Functions in the Large  $x$  Large  $Q^2$  Kinematic Region in Neutrino Deep Inelastic Scattering*, Ph.D. Dissertation for the University of Cincinnati, 1997 (unpublished).
  - [3] R.L. Jaffe, *Phys. Rev.* 50, 228 (1983).
  - [4] D.F. Geesaman, K. Saito, and A.W. Thomas, *Ann. Rev. Part. Sci.* 45, 337-90 (1995).
  - [5] W.C. Leung, et al., *Phys. Lett. B* 317, 665 (1993). Quintas, P.Z., et al., *Phys. Rev. Lett.* 71, 1307 (1993).
  - [6] B.J. King, et al., *Nucl. Instrum. Methods A* 302, 254-260 (1990). W.K. Sakumoto, et al., *Nucl. Instrum. Methods A* 294, 179-192 (1990).
  - [7] A.J. Buras, and K.J.F. Gaemers, *Nucl. Phys. B* 132, 249 (1978).
  - [8] J. Botts et al., *Phys. Lett. B* 304, 159 (1993).
  - [9] A. Bodek, and J.L. Ritchie, *Phys. Rev. D* 23, 1070 (1980). A. Bodek and J.L. Ritchie, *Phys. Rev. D* 24, 1400 (1981).
  - [10] L. Frankfurt and M. Strikman, *Phys. Rep.* 76, 215 (1981).